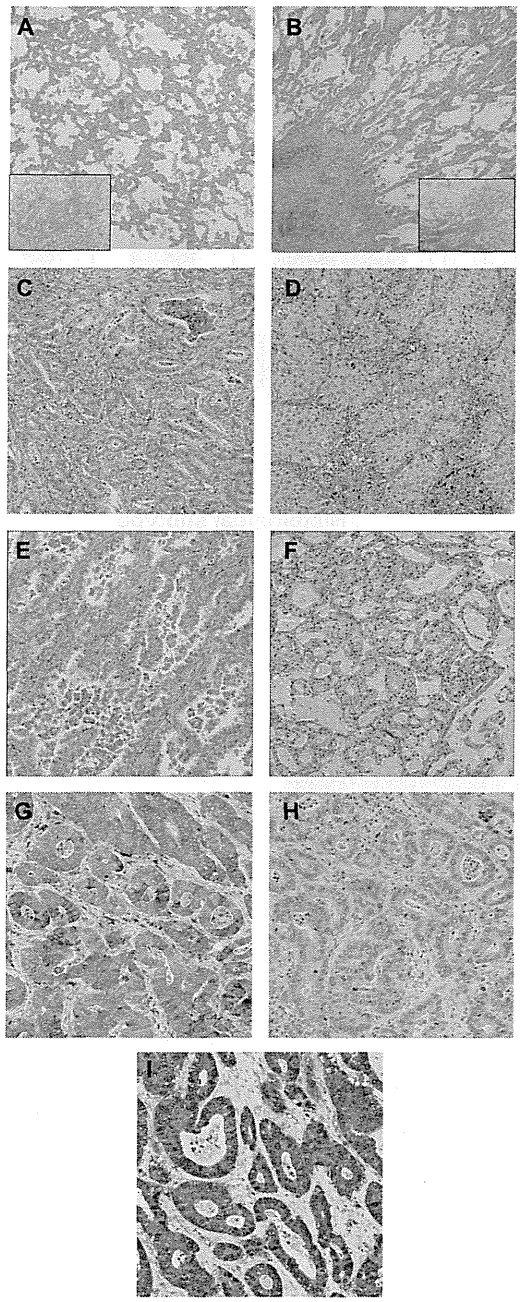

Figure 1 Images of predominant growth patterns and immunohistochemical staining of ALDH1, AK1C1, and AK1C3. (**A**) Adenocarcinoma in situ, (**B**) minimally invasive adenocarcinoma, (**C**) acinar, (**D**) solid, (**E**) micropapillary, and (**F**) mucinous predominant adenocarcinoma. Also shown are immunohistochemical staining images for (**G**) ALDH1A1, (**H**) AK1C1, and (**I**) AK1C3. These slides correspond to the acinar predominant adenocarcinoma shown in Figure 1C.
Abbreviations: ALDH1A1, aldehyde dehydrogenase 1A1; AK1C1, aldo-keto reductase 1C family member 1; AK1C3, aldo-keto reductase 1C family member 3.

one-way analysis of variance, with the Tukey-Kramer multiple comparison post hoc test, was used to allow for unequal sample sizes and determine whether there was a significant difference between the mean immunohistochemical extensiveness according to the predominant histologic pattern of ADC. A P-value of less than 0.05 was considered to indicate a statistically significant difference. The Stat-view 5.0 software package was used to perform the statistical analysis (SAS Institute Inc., Cary, NC, USA).

Results

Predominant growth pattern and ALDH1A1, AK1C1, and AK1C3 expression

All resected specimens were reclassified according to the IASLC/ATS/ERS classification. Representative results are shown in Figure 1. Reclassification of the 103 specimens resulted in three adenocarcinoma in situ (2.9%, Figure 1A), six minimally invasive adenocarcinoma (5.8%, Figure 1B), and 94 invasive ADCs (91.3%). Invasive ADCs were further divided into: lepidic predominant, eight (7.8%); papillary predominant, 39 (37.9%); acinar predominant, ten (9.7%, Figure 1C); solid predominant, 27 (26.2%, Figure 1D); and micropapillary predominant, five (4.9%, Figure 1E). Specific ADC subtypes included four invasive mucinous ADCs (3.9%, Figure 1F) and one enteric ADC (1.0%). Representative examples of immunohistochemical stains for ALDH1A1, AK1C1, and AK1C3 are shown in Figure 1G–I, respectively. This corresponds to the acinar predominant ADC shown in Figure 1C. These CSC-related markers were expressed mainly in the cytoplasm and membrane of the tumor cells. Tumor cells in 68 (66.0%) of the 103 specimens were positive for ALDH1A1, tumor cells in 64 (62.7%) were positive for AK1C1, and tumor cells in 87 (86.1%) were positive for AK1C3.

Correlation between CSC-related marker expression and predominant ADC subtypes

We investigated the correlation between expression of ALDH1A1, AK1C1, and AK1C3 and each predominant subtype. Figure 2 presents the immunohistochemical extensiveness results for adenocarcinoma in situ–minimally invasive ADC (noninvasive ADC), lepidic, acinar, solid, papillary, micropapillary, and mucinous ADC. Immunoreactivities with the percentage of immunopositive areas show that the mean expression of ALDH1A1 in papillary predominant ADCs was significantly higher than that in solid predominant ADCs (Figure 2A, $P<0.05$). On the other hand, Figure 2B shows that papillary predominant ADCs had significantly lower expression of AK1C1 compared with noninvasive or solid predominant ADCs ($P<0.05$). No significant

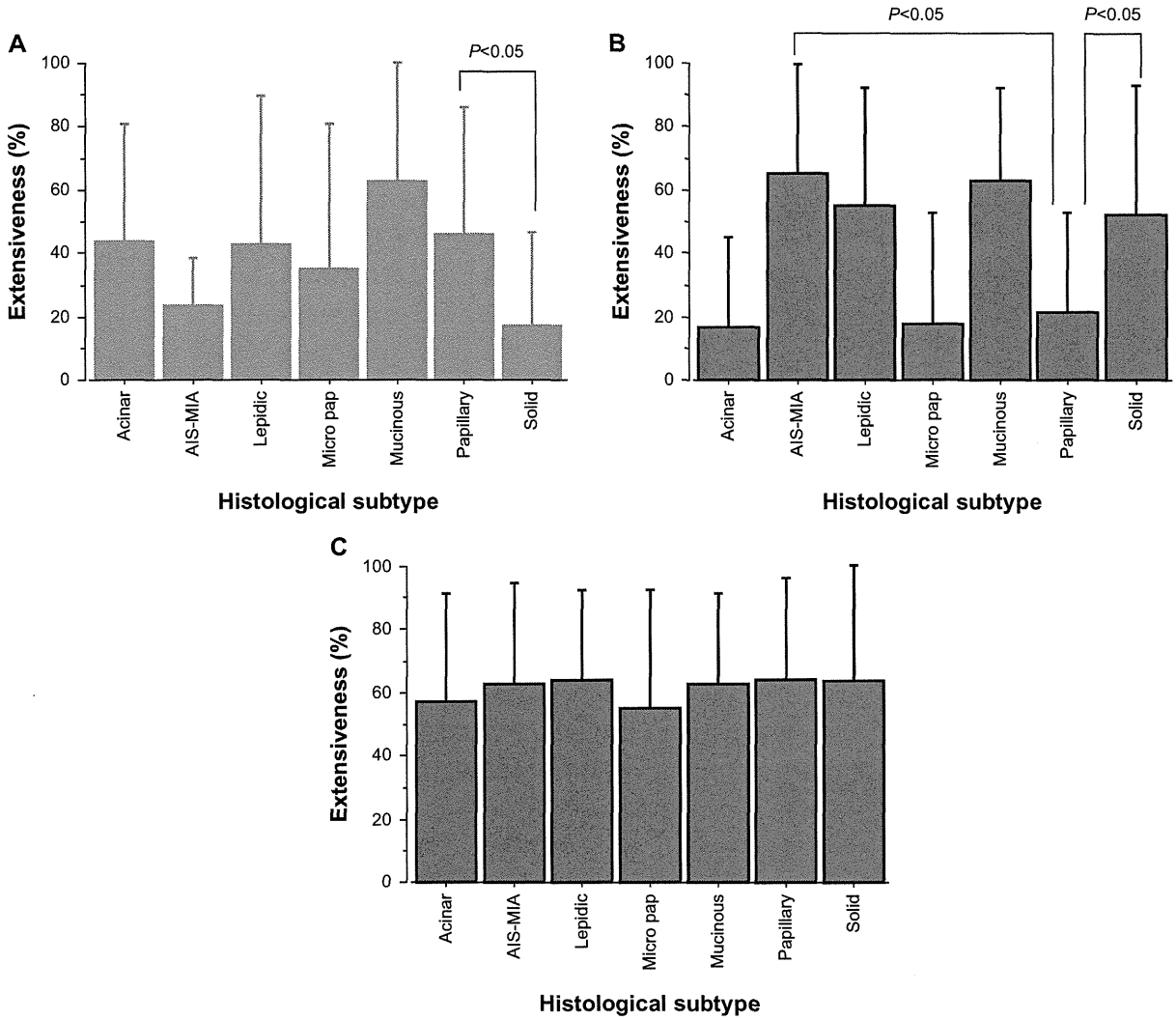

Figure 2 Cancer stem cell-related marker expression in each histologic subtype of lung adenocarcinoma. An overview of the correlation between ALDH1A1, AK1C1, and AK1C3 expression and predominant subtypes is provided. The bars reflect the mean ± standard error of the mean for extensiveness of the immunopositive area for each of the growth patterns. (**A**) Mean expression of ALDH1A1 in papillary predominant adenocarcinomas is significantly higher than that in solid predominant adenocarcinomas ($P<0.05$). (**B**) Papillary predominant adenocarcinomas had significantly lower expression of AK1C1 compared with noninvasive or solid predominant adenocarcinomas ($P<0.05$). (**C**) No significant difference in AK1C3 expression was found for any predominant subtype.

Abbreviations: AIS, adenocarcinoma in situ; MIA, minimally invasive adenocarcinoma; ALDH1A1, aldehyde dehydrogenase 1A1; AK1C1, aldo-keto reductase 1C family member 1; AK1C3, aldo-keto reductase 1C family member 3.

difference in AK1C3 expression was found between any of the predominant subtypes (Figure 2C).

Patient characteristics and survival analyses

The median follow-up for survivors was 8.9 years. Table 1 shows the 5-year overall survival proportions according to clinicopathologic characteristics in 103 patients with lung ADC. On univariate analysis, pathologic stage, tumor size, lymph node involvement, histologic vascular invasion, pleural invasion, and ALDH1A1 immunoreactivity status were found to be significantly associated with survival outcome. The 5-year overall survival proportions of patients with ALDH1A1-positive status and ALDH1A1-negative status were 77.9% and 62.2%, respectively. Patients with an ALDH1A1-positive status had longer overall survival than those with an ALDH1A1-negative status ($P=0.002$, Figure 3), whereas staining with AK1C1 and AK1C3 had no prognostic significance ($P=0.249$ and $P=0.113$, respectively). A multivariate Cox proportional hazards model demonstrated that larger tumor size (hazards ratio 1.899, $P=0.044$), lymph node metastasis (hazards ratio 2.702, $P=0.005$), and low expression of ALDH1A1 immunoreactivity (hazards ratio 3.218, $P<0.001$) were independently associated with unfavorable overall survival (Table 2).

Table 1 Patient characteristics and univariate analysis of overall survival

Variable	Cases, n (%)	5-year OS rate	*P*-value
Overall	103	72.6%	
Age (years, median 65)			
<65	50 (49)	73.6%	
≥65	53 (51)	71.7%	0.416
Gender			
Male	57 (55)	68.0%	
Female	46 (45)	78.3%	0.226
Smoking status			
Smoker	59 (57)	67.8%	
Never smoker	44 (43)	79.2%	0.458
p Stage			
I	78 (76)	83.2%	
II	12 (12)	66.7%	(Stage I
III	11 (11)	27.3%	versus II–IV)
IV	2 (2)	50.0%	<0.001
Tumor size			
≤3.0 cm	61 (59)	80.0%	
>3.0 cm	42 (41)	61.9%	0.006
Lymph node metastasis			
Absent	82 (80)	81.5%	
Present	21 (20)	38.1%	<0.001
Differentiation			
Well or moderate	72 (70)	76.2%	
Poor	31 (30)	61.3%	0.304
IASLC/ATS/ERS classification			
AIS	3 (3)	100%	
MIA	6 (6)	100%	
Lepidic	8 (8)	87.5%	
Papillary	39 (38)	64.1%	
Acinar	10 (10)	100%	
Micropapillary	5 (5)	40.0%	
Solid	27 (26)	66.7%	
Mucinous	4 (4)	100%	
Other (enteric)	1 (1)	100%	
Vascular invasion			
Absent	43 (42)	81.1%	
Present	56 (58)	64.3%	0.001
Pleural invasion			
Absent	82 (80)	79.3%	
Present	21 (20)	45.7%	0.005
Adjuvant chemotherapy			
With	40 (39)	75.0%	
Without	63 (61)	71.1%	0.337
ALDH1A1 expression			
<5% positive cells	35 (34)	62.2%	
≥5% positive cells	68 (66)	77.9%	0.002
AK1C1 expression			
<5% positive cells	38 (37)	71.1%	
≥5% positive cells	64 (63)	74.7%	0.249
AK1C3 expression			
<5% positive cells	14 (14)	61.9%	
≥5% positive cells	87 (86)	74.7%	0.113

Abbreviations: AIS, adenocarcinoma in situ; MIA, minimally invasive adenocarcinoma; OS, overall survival; IASLC, International Association for the Study of Lung Cancer; ATS, American Thoracic Society; ERS, European Respiratory Society; ALDH1A1, aldehyde dehydrogenase 1A1; AK1C1, aldo-keto reductase 1C family member 1; AK1C3, aldo-keto reductase 1C family member 3.

Correlation between clinicopathologic features and ALDH1A1 expression

ALDH1A1 expression status was the most powerful prognostic indicator in this cohort. Therefore, we examined correlations between ALDH1A1-positive cases and clinicopathologic features (Table 3). The ALDH1A1-positive cases were significantly associated with less poorly differentiated ADC (P=0.013). No other clinicopathologic factors were correlated with these cases.

Discussion

We set out to determine whether ALDH1A1 immunoreactivity status was the most powerful independent prognostic factor for overall survival in lung ADC, and expression of each CSC-related marker varied in histologic subtype according to the IASLC/ATS/ERS classification. To the best of our knowledge, the association between CSC-related marker expression and the IASLC/ATS/ERS classification has not been previously investigated in patients for all stages of lung ADC.

The three markers examined in this study have been previously reported as candidate CSC-related markers in different types of tumors. ALDH1 is a detoxifying enzyme responsible for oxidation of intracellular aldehydes. The ALDH isoform, ALDH1A1, has been shown to play a role in drug resistance, and its activity has been used to identify stem-like subsets in human hematopoietic cancers and other solid tumors.[18–25] Previously published studies reported that overexpression of ALDH1A1 correlated with poor prognosis in lung cancer.[12,15] Theoretically, a high proportion of CSCs in the tumor should be associated with an unfavorable prognosis. However, our results show that increased expression of ALDH1A1 correlated with more favorable overall survival, so are very much in conflict with the above mentioned literature. One of the reasons for this discrepancy may lie in the methodologic differences or different cutoff values used for distinguishing between positive and negative CSC-related marker expression. Our method was based on evaluating whole-mount tissue slides and 66% of tumor specimens were ALDH1A1-positive, whereas the results of the previous studies based on tissue microarrays showed only 29%–45% of tumor samples to be positive with a mixture of ADCs and other histology.[12,15] Although the current study population was too small to draw any statistically definite conclusions, the methodology of using tissue microarray may prevent detailed observation and increase the rate of false-negative results. Kahlert et al reported that low immunohistochemical expression of ALDH1 in pancreatic cancer was associated with

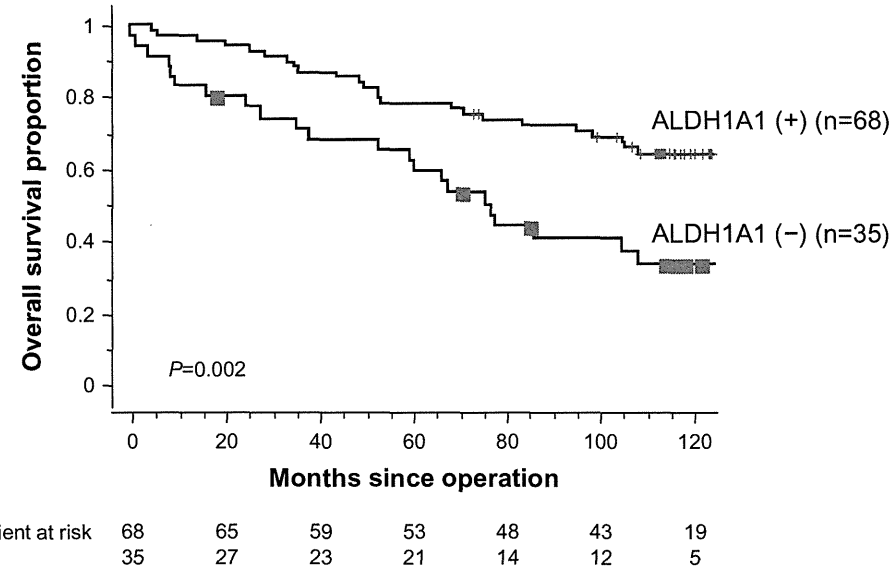

Figure 3 Kaplan–Meier overall survival curves by ALDH1 expression. Five-year overall survival for ALDH1A1-positive and ALDH1A1-negative patients was 77.9% and 62.2%, respectively (*P*=0.002).
Abbreviation: ALDH1A1, aldehyde dehydrogenase 1A1.

poor survival,[26] and Chang et al demonstrated that ALDH1 expression correlated with a favorable prognosis in ovarian cancer,[27] being in line with our study results. It seems possible that one CSC marker from one organ or specific histology is not necessarily useful for identifying CSCs from other organs or histology. In lung ADC, ALDH1 may not be purely a CSC marker but the prognostic marker playing some pivotal role in biologic tumor behavior.

ALDH1A1-positive ADCs demonstrated a significant correlation with less poorly differentiated ADCs, and the frequency of ALDH1A1-positive tumors in papillary predominant ADCs was higher than in solid predominant ADCs.

Table 2 Multivariate analysis of overall survival

Variable	Hazard ratio	95% CI	*P*-value
Tumor size			
≤3.0 cm	1	1.017–3.546	0.044
>3.0 cm	1.899		
Lymph node metastasis			
Absent	1	1.354–5.392	0.005
Present	2.702		
Vascular invasion			
Absent	1	0.897–3.868	0.095
Present	1.863		
Pleural invasion			
Absent	1	0.873–3.831	0.110
Present	1.829		
ALDH1A1 expression			
<5% positive cells	3.218	1.674–6.188	<0.001
≥5% positive cells	1		

Abbreviations: ALDH1A1, aldehyde dehydrogenase 1A1; CI, confidence interval.

These results suggest that ALDH1A1 may play some role in essential morphogenic functions in lung ADC, and ALDH1A1-positive tumors may indicate lower biological aggressiveness.

Aldo-keto reductase (AKR) enzymes comprise a functionally diverse gene family.[28] In humans, four AKR1C isoforms have been identified. Of these, AK1C1 and AK1C3 are known to be cytosolic oxidoreductases that are involved in reduction of progesterone to the inactive form, 20-alpha hydroxyprogesterone, and the metabolism of steroids and prostaglandins with multispecificity, respectively.[29–31] Although neither CSC-related immunoreactivity marker had prognostic significance, predominantly solid ADCs had significantly higher expression of AK1C1 when compared with acinar or papillary predominant ADCs.

The prognostic value of the IASLC/ATS/ERS classification of lung ADC has been validated in several retrospective studies.[3,5–7] Yoshizawa et al recently reported a significant correlation between *EGFR* mutations and adenocarcinoma in situ/minimally invasive adenocarcinoma/lepidic/papillary subtypes, and *KRAS* mutation and mucinous subtypes.[6] Kadota et al demonstrated that immunoreactions of thyroid transcription factor-1 differ depending on the predominant structural subtype.[32] In the current study, the histologic subtype appeared to be correlated with specific CSC-related marker expression. The novel classification of lung ADC has important implications, not just for predicting patient prognosis, but also for genetic alterations and molecular biology, and

Table 3 Correlation between ALDH1A1 expression and clinicopathologic characteristics

Variable	ALDH1A1 expression		*P*-value
	<5% positive cells	≥5% positive cells	
Overall	35	68	
Age (years, median 65)			
<65	18	32	
≥65	17	36	0.674
Gender			
Male	18	39	
Female	17	29	0.567
Smoking status			
Ever smoker	20	39	
Never smoker	15	29	0.984
p Stage			
I	24	54	
II	3	9	(I versus II–IV)
III	7	4	
IV	1	1	0.224
Tumor size			
≤3.0 cm	21	40	
>3.0 cm	14	28	0.908
Lymph node metastasis			
Absent	25	57	
Present	10	11	0.139
Differentiation			
Well or moderate	19	53	
Poor	16	15	0.013
IASLC/ATS/ERS classification			
AIS	1	2	
MIA	0	6	
Lepidic	4	4	
Papillary	10	29	
Acinar	2	8	(AIS-MIA versus invasive ADC)
Micropapillary	2	3	
Solid	15	12	0.129
Vascular invasion			
Absent	12	31	
Present	23	33	0.174
Pleural invasion			
Absent	28	54	
Present	7	14	0.944
Adjuvant chemotherapy			
With	15	25	
Without	20	43	0.548

Abbreviations: ADC, adenocarcinoma; AIS, adenocarcinoma in situ; MIA, minimally invasive adenocarcinoma; IASLC, International Association for the Study of Lung Cancer; ATS, American Thoracic Society; ERS, European Respiratory Society; ALDH1A1, aldehyde dehydrogenase 1A1.

plays a pivotal role as a common language between oncologists/pulmonologists, pathologists, radiologists, molecular biologists, and thoracic surgeons.

In conclusion, although this study is limited because the number of patients was relatively small, the expression of ALDH1A1 is an independent predictor of overall survival. Moreover, the frequency of ALDH1A1-positive ADCs that were papillary predominant was higher than for solid predominant, and AK1C1 expression was found to be significantly lower in papillary predominant ADCs than in noninvasive or solid predominant ADCs, suggesting that the comprehensive histologic subtyping approach in the IASLC/ATS/ERS classification provides new molecular biology insights regarding CSC theory.

Acknowledgments

The authors are indebted to Professor James M Vardaman of Waseda University and Professor J Patrick Barron, Chairman of the Department of International Medical Communications of Tokyo Medical University, for their editorial review of the English manuscript. This study was supported by grants from the Japanese Ministry of Education, Culture, Sports, Science and Technology (24592104), the Japanese Ministry of Health, Labour and Welfare (22101601), and the Tokyo Medical University of 2012.

Disclosure

All authors report they have no conflicts of interest associated with this study.

References

1. Jemal A, Siegel R, Xu J, et al. Cancer statistics, 2010. *CA Cancer J Clin.* 2010;60:277–300.
2. Travis WD, Brambilla E, Noguchi M, et al. International Association for the Study of Lung Cancer/American Thoracic Society/European Respiratory Society international multidisciplinary classification of lung adenocarcinoma. *J Thorac Oncol.* 2011;6:244–285.
3. Warth A, Muley T, Meister M, et al. The novel histologic International Association for the Study of Lung Cancer/American Thoracic Society/European Respiratory Society classification system of lung adenocarcinoma is a stage-independent predictor of survival. *J Clin Oncol.* 2012;30:1438–1446.
4. Xu L, Tavora F, Battafarano R, et al. Adenocarcinomas with prominent lepidic spread: retrospective review applying new classification of the American Thoracic Society. *Am J Surg Pathol.* 2012;36:273–282.
5. Yoshizawa A, Motoi N, Riely GJ, et al. Impact of proposed IASLC/ATS/ERS classification of lung adenocarcinoma: prognostic subgroups and implications for further revision of staging based on analysis of 514 stage I cases. *Mod Pathol.* 2011;24:653–664.
6. Yoshizawa A, Sumiyoshi S, Sonobe M, et al. Validation of the IASLC/ATS/ERS lung adenocarcinoma classification for prognosis and association with EGFR and KRAS gene mutations: analysis of 440 Japanese patients. *J Thorac Oncol.* 2013;8:52–61.
7. Russell PA, Wainer Z, Wright GM, et al. Does lung adenocarcinoma subtype predict patient survival? A clinicopathologic study based on the new International Association for the Study of Lung Cancer/American Thoracic Society/European Respiratory Society international multidisciplinary lung adenocarcinoma classification. *J Thorac Oncol.* 2011;6:1496–1504.
8. Reya T, Morrison SJ, Clarke MF, et al. Stem cells, cancer, and cancer stem cells. *Nature.* 2001;414:105–111.
9. Cai J, Cheng A, Luo Y, et al. Membrane properties of rat embryonic multipotent neural stem cells. *J Neurochem.* 2004;88:212–226.

10. Ginestier C, Hur MH, Charafe-Jauffret E, et al. ALDH1 is a marker of normal and malignant human mammary stem cells and a predictor of poor clinical outcome. *Cell Stem Cell*. 2007;1:555–567.
11. Huang EH, Hynes MJ, Zhang T, et al. Aldehyde dehydrogenase 1 is a marker for normal and malignant human colonic stem cells (SC) and tracks SC overpopulation during colon tumorigenesis. *Cancer Res*. 2009;69:3382–3389.
12. Jiang F, Qiu Q, Khanna A, et al. Aldehyde dehydrogenase 1 is a tumor stem cell-associated marker in lung cancer. *Mol Cancer Res*. 2009;7:330–338.
13. Dozmorov MG, Azzarello JT, Wren JD, et al. Elevated AKR1C3 expression promotes prostate cancer cell survival and prostate cell-mediated endothelial cell tube formation: implications for prostate cancer progression. *BMC Cancer*. 2010;10:672.
14. Seo DC, Sung JM, Cho HJ, et al. Gene expression profiling of cancer stem cell in human lung adenocarcinoma A549 cells. *Mol Cancer*. 2007;6:75.
15. Li X, Wan L, Geng J, et al. Aldehyde dehydrogenase 1A1 possesses stem-like properties and predicts lung cancer patient outcome. *J Thorac Oncol*. 2012;7:1235–1245.
16. Patel M, Lu L, Zander DS, et al. ALDH1A1 and ALDH3A1 expression in lung cancers: correlation with histologic type and potential precursors. *Lung Cancer*. 2008;59:340–349.
17. International Union Against Cancer. *TNM Classification of Malignant Tumours*. 7th ed. Oxford, UK: Wiley-Blackwell; 2009.
18. Hilton J. Role of aldehyde dehydrogenase in cyclophosphamide-resistant L1210 leukemia. *Cancer Res*. 1984;44:5156–5160.
19. Yoshida A, Rzhetsky A, Hsu LC, et al. Human aldehyde dehydrogenase gene family. *Eur J Biochem*. 1998;251:549–557.
20. Tanei T, Morimoto K, Shimazu K, et al. Association of breast cancer stem cells identified by aldehyde dehydrogenase 1 expression with resistance to sequential Paclitaxel and epirubicin-based chemotherapy for breast cancers. *Clin Cancer Res*. 2009;15:4234–4241.
21. Lindahl R. Aldehyde dehydrogenases and their role in carcinogenesis. *Crit Rev Biochem Mol Biol*. 1992;27:283–335.
22. Storms RW, Trujillo AP, Springer JB, et al. Isolation of primitive human hematopoietic progenitors on the basis of aldehyde dehydrogenase activity. *Proc Natl Acad Sci U S A*. 1999;96:9118–9123.
23. Kastan MB, Schlaffer E, Russo JE, et al. Direct demonstration of elevated aldehyde dehydrogenase in human hematopoietic progenitor cells. *Blood*. 1990;75:1947–1950.
24. Hess DA, Meyerrose TE, Wirthlin L, et al. Functional characterization of highly purified human hematopoietic repopulating cells isolated according to aldehyde dehydrogenase activity. *Blood*. 2004;104:1648–1655.
25. Armstrong L, Stojkovic M, Dimmick I, et al. Phenotypic characterization of murine primitive hematopoietic progenitor cells isolated on basis of aldehyde dehydrogenase activity. *Stem Cells*. 2004;22:1142–1151.
26. Kahlert C, Bergmann F, Beck J, et al. Low expression of aldehyde dehydrogenase 1A1 (ALDH1A1) is a prognostic marker for poor survival in pancreatic cancer. *BMC Cancer*. 2011;11:275.
27. Chang B, Liu G, Xue F, et al. ALDH1 expression correlates with favorable prognosis in ovarian cancers. *Mod Pathol*. 2009;22:817–823.
28. Jez JM, Flynn TG, Penning TM. A new nomenclature for the aldo-keto reductase superfamily. *Biochem Pharmacol*. 1997;54:639–647.
29. Hara A, Matsuura K, Tamada Y, et al. Relationship of human liver dihydrodiol dehydrogenases to hepatic bile-acid-binding protein and an oxidoreductase of human colon cells. *Biochem J*. 1996;313(Pt 2):373–376.
30. Lin HK, Jez JM, Schlegel BP, et al. Expression and characterization of recombinant type 2 3 alpha-hydroxysteroid dehydrogenase (HSD) from human prostate: demonstration of bifunctional 3 alpha/17 beta-HSD activity and cellular distribution. *Mol Endocrinol*. 1997;11:1971–1984.
31. Khanna M, Qin KN, Wang RW, et al. Substrate specificity, gene structure, and tissue-specific distribution of multiple human 3 alpha-hydroxysteroid dehydrogenases. *J Biol Chem*. 1995;270:20162–20168.
32. Kadota K, Nitadori J, Sarkaria IS, et al. Thyroid transcription factor-1 expression is an independent predictor of recurrence and correlates with the IASLC/ATS/ERS histologic classification in patients with stage I lung adenocarcinoma. *Cancer*. 2013;119:931–938.

Interactive CardioVascular and Thoracic Surgery 17 (2013) 227–232
doi:10.1093/icvts/ivt120 Advance Access publication 26 April 2013

Virtual segmentectomy based on high-quality three-dimensional lung modelling from computed tomography images

Hisashi Saji[a,*], Tatsuya Inoue[a], Yasufumi Kato[a], Yoshihisa Shimada[a], Masaru Hagiwara[a], Yujin Kudo[a], Soichi Akata[b] and Norihiko Ikeda[a]

[a] Department of Thoracic Surgery, Tokyo Medical University, Tokyo, Japan
[b] Department of Radiology, Tokyo Medical University, Tokyo, Japan

* Corresponding author. Department of Thoracic Surgery, Tokyo Medical University, 6-7-1 Nishishinjuku, Shinjuku-ku, Tokyo 160-0023, Japan. Tel: +81-3-33426111; fax: +81-3-33490326; e-mail: saji-q@ya2.so-net.ne.jp (H. Saji).

Received 13 November 2012; received in revised form 24 February 2013; accepted 27 February 2013

Abstract

OBJECTIVES: The aim of this study was to demonstrate the feasibility and efficacy of a novel simulation software called, virtual segmentectomy.

METHODS: We developed the segmentectomy simulation system, which was programmed to analyse the detailed 3D bronchovascular structure and to predict the appropriate segmental surface and surgical margin, based on lung modelling from CT images.

RESULTS: We have attempted this novel technique for 3 cases of pulmonary metastases and 1 case of multiple lung cancer. For validation, the predicted resection margin was compared with the actual resected specimen. The surgical surface, as estimated by the simulation, was compared with the surface of the specimen and a surgical video. To test its feasibility, the operation time, blood loss, durations of chest tube placement and hospitalization as well as pathological findings were assessed.

CONCLUSIONS: Preoperative simulation and intraoperative guidance by virtual segmentectomy could contribute significantly to determining the most appropriate anatomical segmentectomy and curative resection.

Keywords: 3D computed tomography • Surgical techniques • Lung segmentectomy • Simulation • Computer applications

INTRODUCTION

New technologies can considerably improve preoperative planning, enhance the surgeon's skill, and simplify the approach to complex surgical procedures. Recently, surgical simulation based on preoperative 3D computed tomography (CT) scan has been developed in the fields of head and neck surgery, neurosurgery, orthopaedic surgery and general surgery.

Because of the increasing detection of early small lung cancer lesions due to the expansion of low-dose CT screening, sublobar resections of the lung, including segmentectomy and wedge resection, are becoming common procedures [1]. However, segmentectomy is a complicated operative procedure because of its anatomical complexity, including the high variability of vascular and bronchial structures and the technical difficulty in obtaining an adequate surgical margin due to tumour location and the number of tumours. There have been reports of a recently developed hepatectomy simulation software, regarding its feasibility and efficacy in the fields of both general surgery and liver transplantation [2–5]. This software was designed to analyse detailed 3D vascular structure and to predict liver resection volume and margins. We have developed a segmentectomy simulation system for thoracic called virtual segmentectomy, based on high-quality 3D lung modelling from CT images using the Fujifilm Synapse Vincent system (Fujifilm Corporation, Tokyo, Japan). In this article, we describe 2 representative cases and report the preliminary results of the preoperative and intraoperative assessment via this simulation software in 4 consecutive cases.

TECHNOLOGY

Computed tomography, 3D angiography and bronchial tree

Virtual segmentectomy, surgical simulation of a segmentectomy using 3D lung modelling, was performed with a 64-channel multidetector CT (MDCT) (Light Speed VCT, General Electric Company, CT, USA). A total of 100 ml of contrast agent was injected by a mechanical injector at a rate of 1.5–2.0 ml/s. Scanning parameters used for the contrast examination were as follows: a slice thickness of 1.25 mm, a table displacement of 39.37 mm/rot, and a reconstruction interval of 1.0 mm. Using 3D volume rendering, a solid image was constructed from 1.25-mm data slices of the contrast-enhanced CT images. These digital imaging and communication in medicine data were transferred to a workstation with the Synapse Vincent volume-rendering

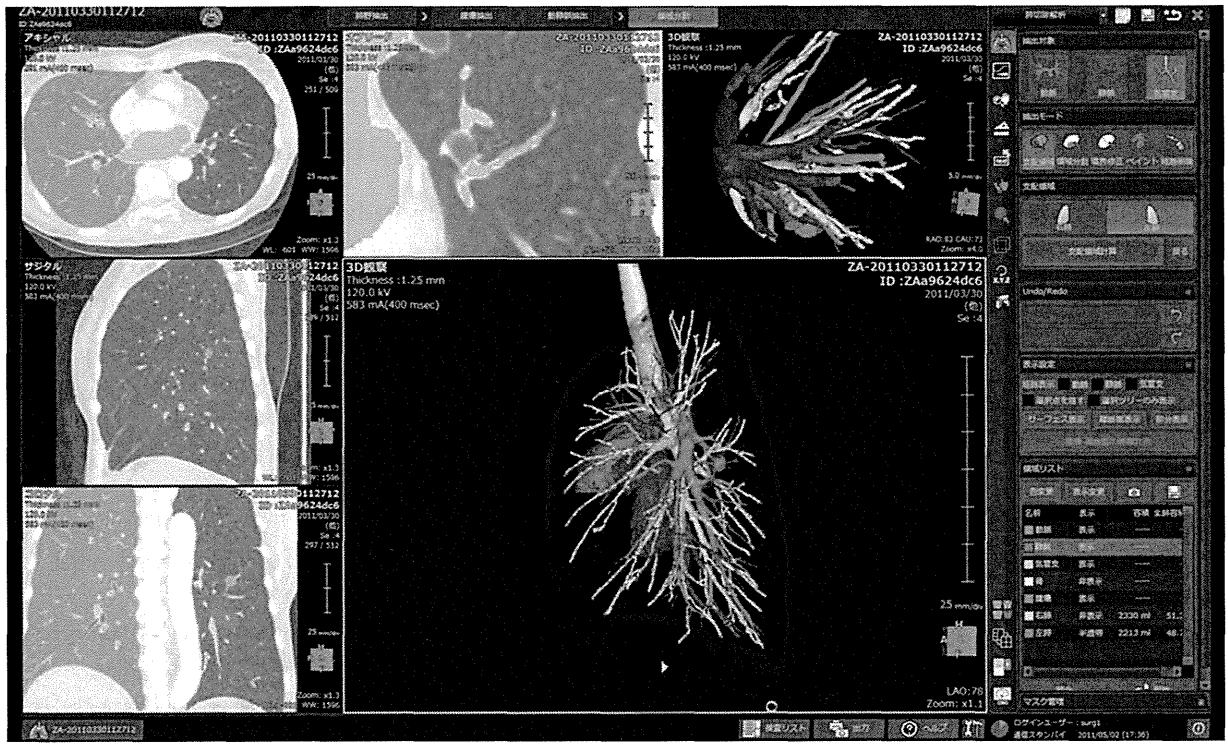

Figure 1: Interface of the lung resection analysis function packaged in Synapse Vincent (Fujifilm).

reconstruction software, which includes a novel 3D image-processing system for the preoperative simulation of segmentectomy. The procedures for 3D reconstruction of the pulmonary vessels and bronchial trees were performed automatically, then further corrected by a thoracic surgeon, taking anatomical variability into account. These procedures took only 5–10 min (Fig. 1).

Preoperative segmentectomy simulation, virtual segmentectomy

Image analysis for the preoperative segmentectomy simulation called virtual segmentectomy was performed using the novel 3D CT image-processing software, including a lung resection analysis function, packaged in Synapse Vincent, developed in collaboration between our department and Fujifilm Corporation. This software has been commercially available since April 2012 and is now being used routinely in our institution. This particular process consisted of the following steps: (i) transfer of CT images to the 3D imaging system; (ii) 3D reconstruction of the tumour, pulmonary vessels, tracheo-bronchial tree and lung parenchyma (Fig. 1); (iii) definition of the segmental bronchi based on the location of the tumour; (iv) calculation of the bronchial ventilation area using an algorithm based on the direction and diameter of the bronchi (Figs 2B and 3B); (v) determination of the sites of resection of the pulmonary vessels, bronchi and inter-segmental veins (Figs 2C and 3E); (vi) calculation of the extent of the surgical margin (Fig. 2D and E) and (vii) visualization of the appropriate segmentectomy surface (Figs 2E and 3E). The 3D CT-guided segmentectomy was initiated by detaching the pulmonary arteries and veins from the pulmonary parenchyma along the shortest route to the target segmental bronchi, according to the preoperative virtual segmentectomy and intraoperative visualization guidance, with an appropriate inter-segmental plane surface (Fig. 3C–E). We performed those operations with double monitor guidance: one was a thoracoscopy television monitor, and the other was a 3D imaging system allowing 3D lung structure and virtual segmentectomy, with which we could reconstruct 3D imaging during operations (Fig. 4).

The simulation system was implemented as a plug-in in the processing workstation (Dell Precision T5500, Windows 7 Professional, 64-bit, 12GB, DDR3 RDIMM).

3D CT-guided segmentectomy

We performed 3D CT-guided segmentectomy for video-assisted thoracoscopic surgery (VATS)-assisted mini-thoracotomy under guidance from both a television monitor and visualization of virtual segmentectomy. Basically, we applied a surgical approach with a combination of muscle-sparing mini-thoracotomy (incision, 4–10 cm) and another incision for an access port of a thoracoscope for video assistance and used mainly direct visualization for the resection of lung parenchyma. The surgeon directly observed the proximal region of the target lobe and individually ligated and dissected the pulmonary arteries and veins from the pulmonary parenchyma along the shortest route to the intended segmental bronchi, according to preoperative virtual segmentectomy and intraoperative 3D CT guidance (Figs 2E, 3C–E). After the segmental bronchi involved with the diseased segment were isolated and divided, the lung was ventilated using selective jet ventilation through a double-lumen tube or directly through mini-thoracotomy into the orifice of the targeted segmental bronchi. The diseased segment was inflated while the preserved segments appeared to collapse and a line formed between the inflated and deflated lung parenchyma, showing the anatomical

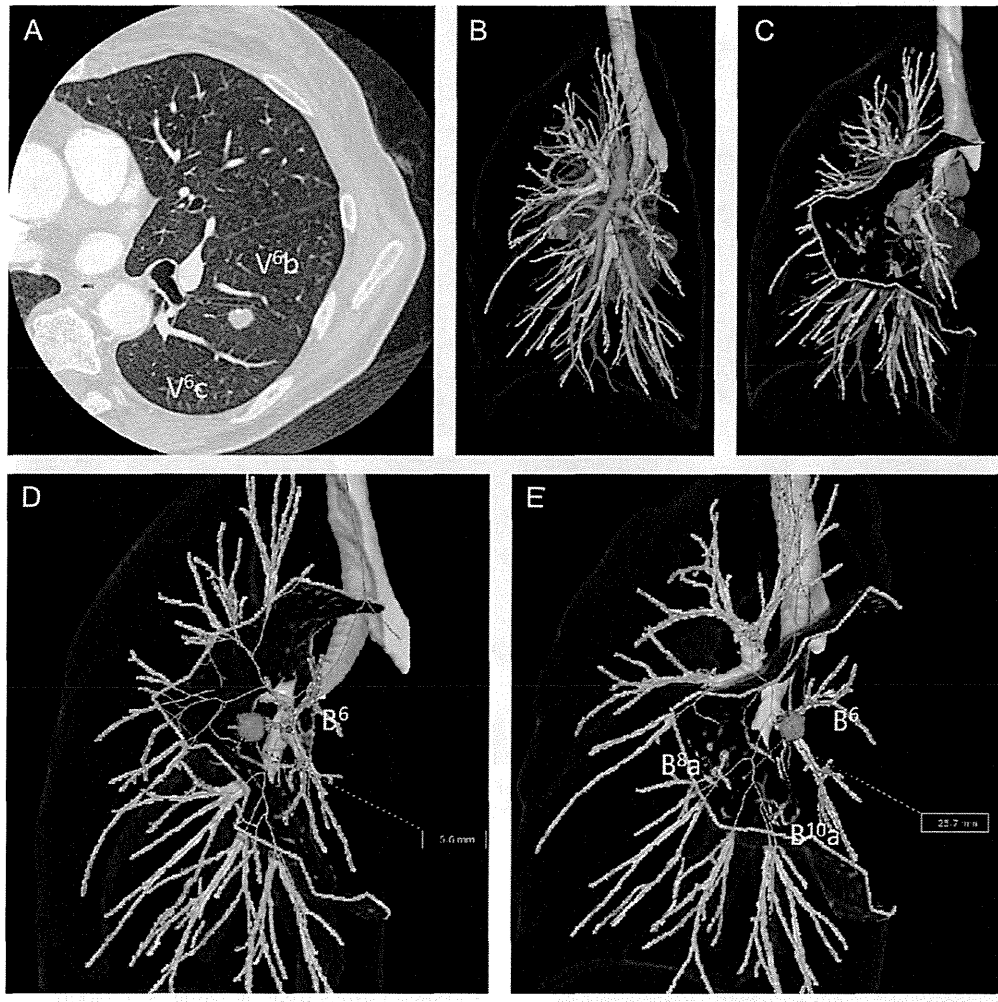

Figure 2: Case 1 (**A** and **B**). According to the virtual S6 segmentectomy, the surgical margin would be estimated to be only 6.6 mm (**D**). While in the virtual segmentectomy of left S6 + S8a + S10a, the appropriate surgical margin was 25.7 mm (**C** and **E**). V^6: superior lower vein, B^6: superior lower bronchus, B^{10}: posterior basal bronchus.

inter-segmental plane. After the segmental bronchi were isolated and dissected using staples or 2-0 silk sutures. Electrocauterization was used to divide the inter-segmental plane along the inflation–deflation line from the peripheral site to the hilum. At the central portion around the hilum, the inter-segmental plane was approached along the inter-segmental vein. We also guided the visualization of 3D CT imaging, including the segmental surface based on virtual segmentectomy simulation to obtain accurate surgical margins. Staplers were only used to divide the inter-segmental plane when the lung was emphysematous, to minimize air leakage. The dissected raw parenchymal surface was sealed with a commercially available fibrin sealant and a bioabsorbable polyglycolic acid felt.

CLINICAL EXPERIENCE

When first using this surgical simulation and navigation system for segmentectomy, we attempted this novel technique on 3 cases of pulmonary metastases and 1 of multiple lung cancer (Table 1). Here, we describe 2 representative cases.

Case 1 was a 69-year old woman with a small solitary pulmonary nodule. Her previous history was mesopharyngeal carcinoma treated with surgical resection followed by chemo-radiotherapy 1 year previously. Chest CT scanning revealed a suspicious metastatic pulmonary tumour located in the superior segment of the left lower lobe (S6) (Fig. 2A). This tumour was very close to pulmonary veins V^6b and V^6c, which are supposed to be inter-segmental pulmonary veins between S6 and the basal segment of the left lower lobe (Fig. 2A). If only the superior segmentectomy of the left lower lobe was performed in this case, this surgical margin was estimated at 6.6 mm, which is <2.0 cm or the maximum tumour size based on the result of the virtual segmentectomy of the superior segment of the left lower lobe (Fig. 2D). Therefore, we performed the extended superior segmentectomy of the left lower lobe according to the pre-operative simulation of the virtual segmentectomy of left S6 + S8a + S10a, obtaining an appropriate surgical margin (25.7 mm), >2.0 cm or the maximum diameter of this tumour (8.8 mm) (Fig. 2E) [6].

Case 2 was a 43-year old man with a 21.2-mm solitary pulmonary nodule in the left S9 + 10 basal segment of the left lower lobe. He had undergone thyroidectomy and thymectomy for thyroid carcinoma and thymic carcinoma 3 and 2 years previously, respectively. This tumour was located on the exact line between S9 and S10 according to the 3D imaging reconstruction

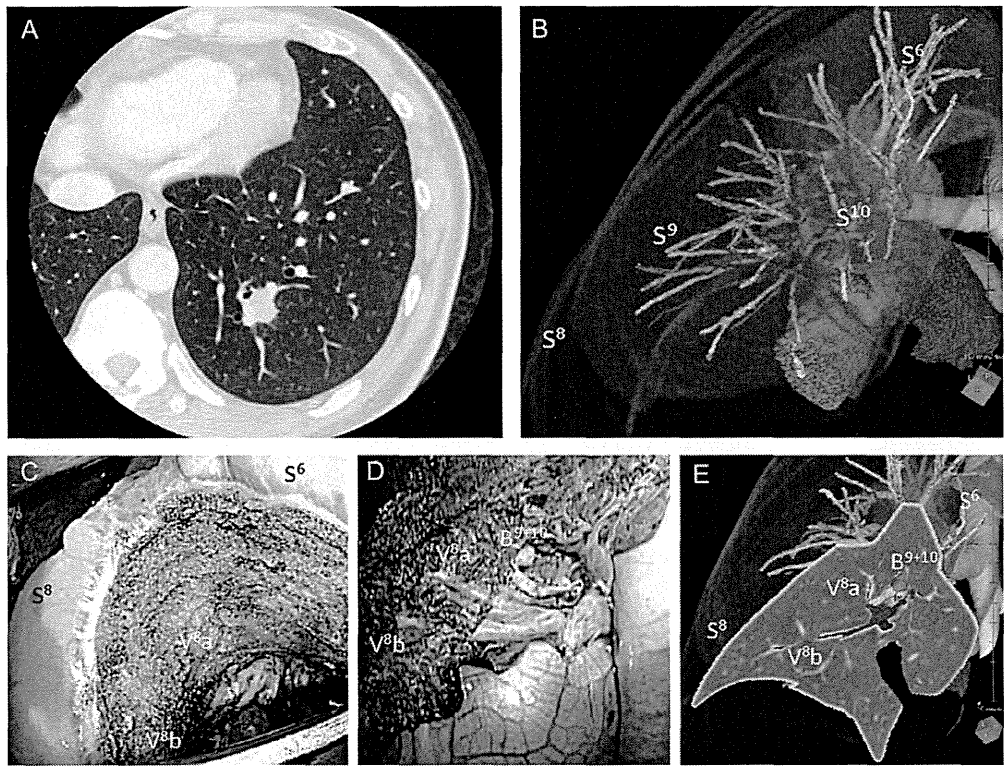

Figure 3: Case 2 (**A** and **B**). Left S9 + S10 segmentectomy under visual guidance of the appropriate virtual segmentectomy (**C–E**). S^6: superior, lower lobe, S^8: anteromedial basal segment, S^9: lateral basal segment, S^{10}: posterior basal segment, V^8: anterior basal pulmonary vein, B^{9+10}: lateral and posterior basal bronchi.

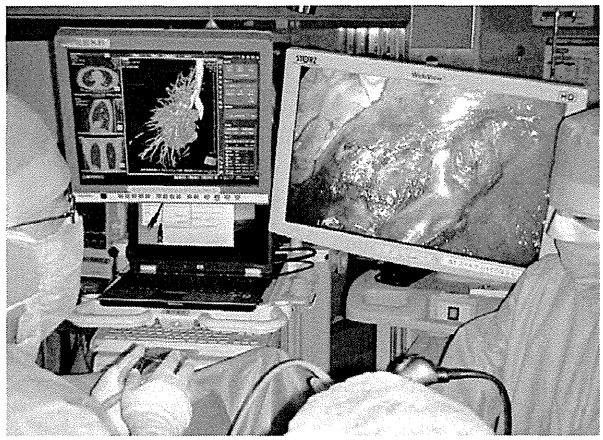

Figure 4: Thoracoscopic surgery using the double monitor guidance system. The thoracoscopy television monitor (right) and the 3D imaging system (left).

of each segmental area of the left lower lobe (Fig. 3B). Therefore, we performed a left S9 + S10 segmentectomy under visual guidance of the appropriate virtual segmentectomy. We used an electrocautery Bovie to dissect the lung parenchyma along the line between inflated and deflated lung, visually guided by the visualization of 3D CT imaging, based on virtual segmentectomy simulation to obtain accurate surgical margins (Fig. 3C–E).

Table 1 shows the preliminary results of surgical outcomes in our 4 consecutive cases. We performed three complex segmentectomies: an extended left S6 segmentectomy, a left S9 + S10 segmentectomy and a right S7 + S8 segmentectomy. We also performed one moderate segmentectomy: a basal segmentectomy of the right lower lobe. After the lung parenchyma was dissected, we sealed it with a commercially available fibrin sealant and a bioabsorbable polyglycolic acid felt in 3 of 4 cases. Operation times were all within 4 h, blood loss volumes ranged from 24 to 120 ml, and chest tubes could be removed on POD 3 in all patients. The durations of hospitalization were from POD 5 to POD 9 without moderate or severe postoperative complications. According to comparisons between 3D CT imaging and pathological findings (Table 2), the extents of preoperative predicted surgical margins by Synapse Vincent tended to be shorter than those of pathological surgical margins, because of deflated resected lung lobes. However, there were no residual tumour cells at the surgical resection margins (confirmed pathologically) and no local recurrence could be detected in any of the 4 cases during the short follow-up period (15–17 months).

COMMENT

The efficacy of 3D CT angiography using MDCT for preoperative assessment for thoracic surgery has been described. Accuracy in depicting individual anatomies of pulmonary vessels and bronchi and preoperative simulation using 3D CT could play an important role in facilitating a safe and complete VATS lobectomy procedure, as has been suggested in some previous reports. Fukuhara *et al.* reviewed 49 consecutive patients with clinical stage I lung cancer and compared intraoperative findings of the pulmonary artery branching pattern with 3D CT angiography images preoperatively obtained using MDCT. According to the results, 95.2% of the pulmonary artery branches were precisely

Table 1: Patient characteristics and surgical outcomes

Case	Age (years)	Sex	Diagnosis	Location	Tumour size (mm)	Operation procedure	Inter-segment	Operation time	Blood loss (ml)	Duration of chest tube placement (POD)	Duration of hospitalization	Morbidity
1	69	F	PM from mesopharyngeal carcinoma	Rt S6	8.8	Lt S6 segmentectomy	Electrocautery	3 h 39 m	120	3	7	None
2	43	M	PM from thymic carcinoma	Lt S9	21.2	Lt S9 + S10 segmentectomy	Electrocautery	3 h 09 m	24	3	9	None
3	77	F	Multiple lung cancer	Rt S8	13.0	Rt S7 + S8 segmentectomy	Electrocautery	3 h 42 m	68	3	5	None
4	59	M	PM from rectal cancer	Rt S9	19.8	Rt basal segmentectomy	Stapler	3 h 52 m	70	3	5	None

Lt: left; PM: pulmonary metastasis; POD: postoperative days; Rt: right.

identified on preoperative 3D CT angiography and conversion to open thoracotomy was not needed. Watanabe *et al.* also reviewed 14 lung cancer cases and stated that 3D CT pulmonary artery navigation may have the potential to increase the safety of surgical procedures [7, 8]. Recently, preoperative identification of the inter-segmental pulmonary vessels and bronchi involved with the resected segment using 3D CT angiography and establishment of a virtual bronchial tree (virtual bronchography) have been demonstrated to be useful tools, enabling the surgeon to perform an accurate anatomical segmentectomy [9, 10]. However, to the best of our knowledge, identifying the inter-segmental surface and calculating appropriate surgical margins by this method have never been established for preoperative procedures for segmentectomy. This article is apparently the first report demonstrating the efficacy of virtual segmentectomy.

It is critical to identify the inter-segmental veins as the boundary lines of the pulmonary segments to determine the lateral surgical margins and to identify the target segmental bronchi as the vertical surgical margins before segmentectomy. However, given the many anatomical variations of pulmonary veins and bronchi, it is difficult to identify the intra-segmental and inter-segmental veins and target segmental bronchi, even by using 3D CT angiography and virtual bronchography. Moreover, it is technically difficult to perform a typical segmentectomy because of the tumour location (Cases 1 and 2). Recently, we have occasionally encountered cases which required multi-segmentectomy for several tumours. Therefore, we have developed the novel segmentectomy simulation system based on high-quality 3D lung modelling from MDCT imaging using the specially developed Synapse Vincent software in collaboration with Fujifilm Corporation.

This particular system consist of the following three novel functions: (i) calculation of the bronchial ventilation area using the algorithm based on the direction and diameter of the bronchi; (ii) visualization of the segmental surface resulting in determination of resected pulmonary artery, vein, bronchi and inter-segmental veins and (iii) calculation of the length of the surgical margin. Based on the preliminary results of our cases, we believe that it could be useful for appropriate anatomical segmentectomy with curative resection. It would enable one to obtain accurate preoperative information regarding not only the relationships among the tumour, the intra-segmental and inter-segmental veins, the target segmental bronchi and pulmonary arteries, but also to visualize the inter-segmental plane surface and secure surgical margins. Moreover, intraoperative visualization guidance of the inter-segmental surface, including intra-segmental and inter-segmental veins, target pulmonary arteries, and bronchi could help thoracic surgeons perform accurate anatomical segmentectomy and curative resection. Additional applications of this novel system include preoperative simulation of multi-segmentectomy for synchronous or metachronous multiple pulmonary tumours and visual guidance for robotic surgeries.

In this preliminary study, we first attempted to demonstrate the usefulness of virtual segmentectomy based on high-quality 3D lung modelling from conventional multidetector CT images to compare intraoperative findings of the pulmonary artery, pulmonary vein and bronchial branching patterns and visualization of the segmental surface. Therefore, we basically performed hybrid VATS to make an accurate assessment not only on a television monitor that provides a 2D view, but also for direct observation using mini-thoracotomy with a real 3D view. In our next study, we will perform complete VATS segmentectomy using this novel technology.

Table 2: Comparisons between 3D CT imaging and pathological findings

Case	Vincent tumour size (CT) (mm)	Pathological tumour size (mm)	Vincent surgical margin length (mm)	Pathological surgical margin length (mm)	Pathological surgical margin	Follow-up (months)	Local recurrence
1	8.8	11.0	12.4	9.8	Negative	14	None
2	21.2	20.0	15.0	10.0	Negative	14	None
3	13.0	13.0	20.6	12.0	Negative	13	None
4	19.8	18.0	30.0	25.0	Negative	12	None

It is critical to obtain an adequate surgical margin for pulmonary malignant tumours, particularly for primary lung cancer. The Vincent surgical margins are overestimated, as evidenced by the pathological margins (Table 2). As this is a preliminary study with a small number of sample cases, we are currently evaluating more cases and assessing detailed information. Because we are more familiar with using this novel technology and performing segmentectomy in many cases with much more inflated target segments, the discrepancies between the Vincent surgical margin and the pathological surgical margin is decreasing.

We understand that a major limitation remains in this system. Virtual visualization of the segmentectomy resection line consisted of the border of the inflated lung, whereas the lung was, in reality, deflated during actual surgical procedures. Further technical development is needed to improve this limitation.

We describe the benefit of virtual segmentectomy, a novel surgical simulation system based on high-quality 3D lung modelling, including vascular and bronchial structures. Preoperative determination of the branches of the pulmonary vessels and segmental bronchi branches and the anatomical inter-segmental surface estimated by the inflated area of segmental bronchi is possible by visualization. Moreover, a sufficient surgical margin from the tumour can be estimated. This new technology appears useful for thoracic surgeons to perform appropriate anatomical segmentectomy and curative resection. Furthermore, we are currently performing a prospective clinical study to demonstrate the efficacy of this novel system for small peripheral primary lung cancer lesions.

ACKNOWLEDGEMENTS

We are indebted to Clifford A. Kolba, Edward F. Barroga and J. Patrick Barron, Department of International Medical Communications of Tokyo Medical University, for their editorial review of the English manuscript.

FUNDING

This study was supported by a Grant-in-Aid for Scientific Research, Japan Society for the Promotion of Science (24592104), and Ministry of Education, Culture, Sports, Science and Technology, Japan.

Conflict of interest: Hisashi Saji and Norihiko Ikeda have given remunerated lectures for Fujifilm. No author received research funding and all had full control of the study design, methods used, outcome parameters, data analysis and production of the written report.

REFERENCES

[1] Sakata R, Fujii Y, Kuwano H. Thoracic and cardiovascular surgery in Japan during 2009: annual report by the Japanese Association for Thoracic Surgery. Gen Thorac Cardiovasc Surg 2011;59:636–67.
[2] Yamanaka J, Saito S, Fujimoto J. Impact of preoperative planning using virtual segmental volumetry on liver resection for hepatocellular carcinoma. World J Surg 2007;31:1249–55.
[3] Saito S, Yamanaka J, Miura K, Nakao N, Nagao T, Sugimoto T *et al.* A novel 3D hepatectomy simulation based on liver circulation: application to liver resection and transplantation. Hepatology 2005;41:1297–304.
[4] Lang H, Radtke A, Hindennach M, Schroeder T, Fruhauf NR, Malago M *et al.* Impact of virtual tumor resection and computer-assisted risk analysis on operation planning and intraoperative strategy in major hepatic resection. Arch Surg 2005;140:629–38; discussion 638.
[5] Yamanaka J, Saito S, Iimuro Y, Hirano T, Okada T, Kuroda N *et al.* The impact of 3-D virtual hepatectomy simulation in living-donor liver transplantation. J Hepatobiliary Pancreat Surg 2006;13:363–9.
[6] Sawabata N, Ohta M, Matsumura A, Nakagawa K, Hirano H, Maeda H *et al.* Optimal distance of malignant negative margin in excision of non-small cell lung cancer: a multicenter prospective study. Ann Thorac Surg 2004;77:415–20.
[7] Watanabe S, Arai K, Watanabe T, Koda W, Urayama H. Use of three-dimensional computed tomographic angiography of pulmonary vessels for lung resections. Ann Thorac Surg 2003;75:388–92; discussion 392.
[8] Fukuhara K, Akashi A, Nakane S, Tomita E. Preoperative assessment of the pulmonary artery by three-dimensional computed tomography before video-assisted thoracic surgery lobectomy. Eur J Cardiothorac Surg 2008;34:875–7.
[9] Oizumi H, Endoh M, Takeda S, Suzuki J, Fukaya K, Sadahiro M. Anatomical lung segmentectomy simulated by computed tomographic angiography. Ann Thorac Surg 2010;90:1382–3.
[10] Shimizu K, Nakano T, Kamiyoshihara M, Takeyoshi I. Segmentectomy guided by three-dimensional computed tomography angiography and bronchography. Interact CardioVasc Thorac Surg 2012;15:194–6.

Lung Cancer 81 (2013) 187–193

Contents lists available at SciVerse ScienceDirect

Lung Cancer

journal homepage: www.elsevier.com/locate/lungcan

Proposal on incorporating blood vessel invasion into the T classification parts as a practical staging system for stage I non-small cell lung cancer

Yujin Kudo[a,*], Hisashi Saji[a], Yoshihisa Shimada[a], Jun Matsubayashi[b], Toshitaka Nagao[b], Masatoshi Kakihana[a], Jitsuo Usuda[a], Naohiro Kajiwara[a], Tatsuo Ohira[a], Norihiko Ikeda[a]

[a] Division of Thoracic Surgery, Department of Surgery, Tokyo Medical University, Japan
[b] Department of Anatomic Pathology, Tokyo Medical University, Japan

ARTICLE INFO

Article history:
Received 10 March 2013
Received in revised form 10 April 2013
Accepted 14 April 2013

Keywords:
Non-small cell lung cancer
Blood vessel invasion
TNM classification
Vascular invasion
Elastica van Gieson stain
Prognostic factor

ABSTRACT

Background: We investigated blood vessel invasion (BVI) as a possible negative prognostic factor in patients with stage I non-small cell lung cancer (NSCLC) according to the 7th edition of the TNM classification.

Methods: Between 1999 and 2007, a total of 694 consecutive patients with pathological stage I NSCLC underwent complete resection with systematic lymph node dissection at Tokyo Medical University Hospital. All sections of the specimens were stained by Elastica van Gieson to visualize elastic fibers and were examined to determine the prognostic symptoms of BVI. We statistically analyzed the association between BVI and clinicopathologic factors, as well as clinical outcomes.

Results: BVI was detected in 201 patients with stage I NSCLC (29.0%). The 5-year overall survival (OS) rates of the non-BVI and BVI patients were 90.5% and 66.0%, respectively ($p < 0.0001$). BVI was found to be a significant independent prognostic factor by multivariate survival analysis in stage IA and stage IB NSCLC (HR 2.591, $p < 0.001$; HR 2.347, $p = 0.009$, respectively). The 5-year OS rate of patients with BVI was significantly worse than that of patients without BVI in the T1a (94.5% vs 87.5%, $p < 0.0001$), T1b (82.7% vs 65.9%, $p < 0.0001$), and T2a (90.9% vs 61.8%, $p < 0.0001$) subgroups.

Conclusion: We identified the presence of BVI as an independent poor prognostic factor in patients with stage I NSCLC. In the future revision of the TNM staging system, the routine use of elastic fiber stains in pathological evaluations of lung cancer for BVI determination might be recommended, and tumors with BVI should be upstaged to the higher current T staging.

1. Introduction

Non-small cell lung cancer (NSCLC) is one of the most common cancers and a major cause of cancer-related deaths. Pathological stage (p-stage) I NSCLC was observed in about 65% of all surgical cases [1], and these patients have the best chance of cure by surgery alone. Within the stage I designation, however, some clinicopathological characteristics may be associated with poor long-term survival. The 5-year overall survival (OS) rates in resected stage IA and IB NSCLC range from 84% to 87% and from 66% to 74%, respectively, as shown in large-scale Japanese lung cancer studies [1,2], although the 5-year OS rates were approximately more than 95% in p-stage I patients with breast cancer, colon cancer or gastric cancer.

Many studies have been reported to determine various prognostic factors other than the pathological stage, such as sex [3], age [3], smoking history [4], serum level of carcinoembryonic antigen (CEA) [5], extent of operation [3], tumor differentiation [6], tumor size [7], and number of involved lymph nodes [8]. In addition, blood vessel invasion (BVI) has been shown to be a strong independent predictor for p-stage I disease in most studies that adopted this factor as a variable for analyses [7,9–12]. Although BVI has been taken into account in the supplementary TNM staging, BVI is not a descriptor of the T component of the TNM classification. The objective of the present study was to evaluate BVI impact on survival and propose a method of incorporating BVI into T status, in relation with the 7th TNM classification.

2. Materials and methods

2.1. Patient selection

A total of 1234 consecutive patients underwent complete pulmonary resection between January 1999 and December 2007 at

* Corresponding author at: Division of Thoracic Surgery, Department of Surgery, Tokyo Medical University, 6-7-1 Nishishinjuku, Shinjuku-ku, Tokyo 160-0023, Japan. Tel.: +81 03 3342 6111x5070; fax: +81 03 3349 0326.
E-mail address: yjnkudo@gmail.com (Y. Kudo).

0169-5002/$ – see front matter © 2013 Elsevier Ireland Ltd. All rights reserved.
http://dx.doi.org/10.1016/j.lungcan.2013.04.016

Tokyo Medical University Hospital. We defined complete resection as lobectomy or more extensive lung resection with systematic ipsilateral hilar and mediastinal lymph node dissection and with no evidence of residual cancer either macroscopically or microscopically. Of these patients, 847 were pathologically proven to have stage I NSCLC. We excluded patients who had received preoperative chemotherapy, radiotherapy or both, or who had been given a diagnosis of low-grade malignant diseases, including carcinoid, mucoepidermoid carcinoma, and adenoid cystic carcinoma. The remaining 694 patients who were pathologically confirmed to have stage I NSCLC were enrolled in this study. We also reviewed 35 patients with surgically resected pathological node-negative stage IIA NSCLC in order to compare the survival and recurrent rates.

We reviewed the medical records of each patient regarding their clinicopathologic information including age, gender, smoking history, tumor location, operation procedure, histologic type, tumor size, blood vessel invasion, lymphatic permeation, and visceral pleural invasion (VPI). Disease stages were based on the 7th edition of the TNM Classification for Lung and Pleural Tumors of the Union for International Cancer Control (UICC).

After resection, the patients were examined at 3-month intervals for 3 years, then at 6-month intervals for the next 2 years, and thereafter at 1-year intervals, in general. The evaluations included physical examination, chest roentgenogram, chest computed tomography (CT), and tumor marker measurement. Abdominal CT and brain MRI as well as bone scintigraphy were performed every year. Patients with cancer recurrence were carefully divided into 2 groups according to the site of initial relapse: locoregional or distant. The median follow-up period was 4.6 years. The Institutional Review Board of our hospital approved the protocols for data collection and analyses, and waived the need to obtain written informed consent from each patient.

2.2. Histopathologic studies

Histopathologic studies were performed according to World Health Organization criteria. After fixing the specimens in 10% formalin and embedding them in paraffin, sections were stained with hematoxylin and eosin and by Elastica van Gieson (EvG) staining to visualize elastic fibers. Detailed examinations of BVI were routinely performed at our institution. Blood vessels were identified by the presence of erythrocytes in the lumen or an endothelial cell lining or the presence of elastic tissue around larger vessels. Sections stained by EvG were examined for the presence of BVI. The presence of BVI was determined by identifying conspicuous clusters of intravascular cancer surrounded by an elastic fiber layer (Fig. 1). On the other hand, lymphatic permeation was determined to be present when tumor cells floating in lymphatic vessels with no supporting smooth muscles or elastic fibers were identified. We confirmed that lumens within the bronchovascular bundle, subpleural, and intralobular pleural space were lymphatic vessels by immunostaining with anti-D2-40 antibody.

2.3. Statistical analysis

Overall survival (OS) and recurrence-free survival (RFS) were estimated using the Kaplan–Meier method, and differences in survival rates were determined by log-rank analysis. OS was defined as the time elapsed from the date of pulmonary resection to the date of death. RFS was defined as the time elapsed from the date of pulmonary resection to the date of the first recurrence or last follow-up showing no recurrence. The last follow-up observation was censored if the patient was alive or lost to follow-up. Univariate analysis was conducted among the different groups. Categorical variables were analyzed using the chi-square test. Differences between 2 groups were tested using the Mann–Whitney

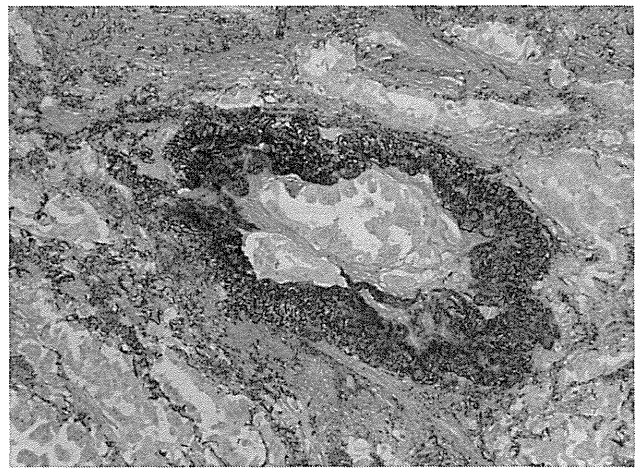

Fig. 1. Elastica van Gieson staining of a tumor with blood vessel invasion (BVI). The presence of BVI was determined by identifying conspicuous clusters of intravascular cancer surrounded by an elastic layer (original magnification, 400×).

U test. Multivariate analysis was performed by the Cox proportional hazards model using the significant factors identified from univariate analysis to examine the association between survival and potential prognostic factors. All *p*-values were two-sided and *p*-values of <0.05 were considered to indicate a statistically significant difference. All statistical calculations were performed using StatView for Windows version 5.0 (SAS Institute Inc., Cary, NC, USA).

3. Results

The characteristics of the patients are shown in Table 1a. BVI was detected in 201 patients (29.0%). The 5-year OS rates of non-BVI and BVI patients were 90.5% and 66.0%, respectively (Fig. 2). The relationship between clinicopathological prognostic factors and BVI is shown in Table 1b. BVI prevalence was significantly higher in men, ever smokers, non-adenocarcinoma, positive lymphatic permeation, positive visceral pleural invasion, and p-stage IB ($p < 0.05$). Tumor size was significantly larger in BVI tumors than in non-BVI tumors ($p < 0.0001$).

In patients with p-stage IA tumors, men, over 70 years old, ever smokers, tumor size over 2 cm in diameter, non-adenocarcinoma, and the presence of BVI were statistically significant poor prognostic factors. Multivariate survival analysis showed that a tumor size over 2 cm in diameter and the presence of BVI were statistically significant independent prognostic factors, as well as ages over 70 years old and non-adenocarcinoma (hazard ratio [HR] = 2.096, $p = 0.0040$; HR = 2.591, $p = 0.0004$, respectively)

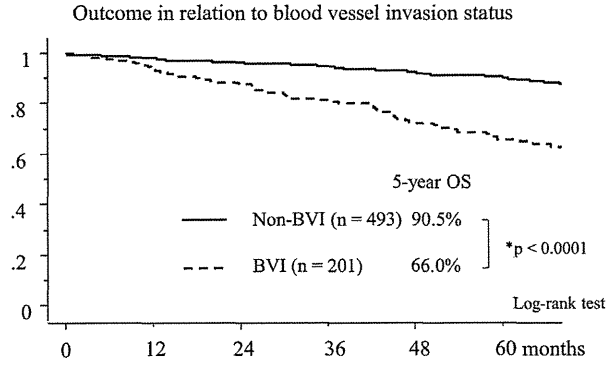

Fig. 2. Survival curves for blood vessel invasion (BVI) and non-BVI. *$p < 0.05$.

Table 1a
Patient characteristics (stage I, $n=694$; stage IIA, $n=35$).

Variable	Number (%)				p value (stage IA vs stage IB)
	All ($n=694$)	Stage IA ($n=423$)	Stage IB ($n=271$)	Stage IIA (T2bN0) ($n=35$)	
Sex					<0.0001*
Men	371(53.5)	200(47.3)	171(63.1)	32(91.4)	
Women	323(46.5)	223(52.7)	100(36.9)	3(8.6)	
Median age (range)	66.0 (22–86)	65.0 (22–86)	67.0 (38–86)	69.0 (48–86)	0.0381*
Smoking history					0.0030*
Never smoker/unknown	315(45.4)	211(49.9)	104(38.4)	5(14.3)	
Ever smoker	379(54.6)	212(50.1)	167(61.6)	30(85.7)	
Tumor location					0.9999
Right	451(65.0)	275(65.0)	176(64.9)	25(71.4)	
Left	243(35.0)	148(35.0)	95(35.1)	10(28.6)	
Operation procedure					0.5355
Lobectomy	669(96.4)	406(96.0)	263(97.0)	33(94.3)	
Bilobectomy	25(3.6)	17(4.0)	8(3.0)	2(5.7)	
Histological type					0.0002*
Adenocarcinoma	568(81.8)	365(86.3)	203(74.9)	18(51.4)	(Ad vs non-Ad)
Squamous cell carcinoma	97(14.0)	47(11.1)	50(18.4)	15(42.9)	
Large cell carcinoma	22(3.2)	8(1.9)	14(5.2)	2(5.7)	
Others	7(1.0)	3(0.7)	4(1.5)	0(0)	
Median tumor size (cm) (range)	2.3 (0.4–5.0)	1.9 (0.4–3.0)	3.5 (0.6–5.0)	6.0 (5.1–7)	<0.0001*
BVI	201(29.0)	73(17.2)	128(47.2)	13 (37.1)	<0.0001*
Lymphatic permeation	237(34.1)	101(23.8)	136(50.2)	17 (48.6)	<0.0001*
VPI	122(17.6)	0(0)	122(45.0)	13 (37.1)	–
pT factor					–
T1a	263(37.9)	263(62.2)	0(0)		
T1b	160(23.1)	160(37.8)	0(0)		
T2a	271(39.0)	0(0)	271(100)		

Ad, adenocarcinoma; non-Ad, other histological types; BVI, blood vessel invasion; VPI, visceral pleural invasion.
* $p<0.05$.

Table 1b
Patient characteristics in the 2 groups according to clinicopathologic factors ($n=694$).

Variable	Number (%)		p-Value [non-BVI vs BVI]
	Non-BVI ($n=493$)	BVI ($n=201$)	
Sex			<0.0001*
Men	228(46.2)	143(71.1)	
Women	265(53.8)	58(28.9)	
Age			0.0705
≤70 years old	143(29.0)	73(36.3)	
>70 years old	350(71.0)	128(63.7)	
Smoking history			<0.0001*
Ever Smoker	229(46.5)	150(74.6)	
Never smoker/unknown	264(53.5)	51(25.4)	
Tumor location			0.9302
Right	321(65.1)	130(64.7)	
Left	172(34.9)	71(35.3)	
Histological type			<0.0001*
Ad	434(88.0)	134(66.7)	
Non-Ad	59(12.0)	67(33.3)	
Operation procedure			0.8225
Lobectomy	476(96.6)	193(96.0)	
Bilobectomy	17(3.4)	8(4.0)	
Median tumor size (cm) (range)	2.0 (0.4–5.0)	3.0 (0.7–5.0)	<0.0001*
Lymphatic permeation			<0.0001*
present	101(20.5)	136(67.7)	
absent	392(79.5)	65(32.3)	
VPI			<0.0001*
present	52(10.5)	70(34.8)	
absent	441(89.5)	131(65.2)	
p-stage			<0.0001*
IA	350(71.0)	73(36.3)	
IB	143(29.0)	128(63.7)	

Non-BVI, without blood vessel invasion; BVI, with blood vessel invasion; Ad, adenocarcinoma; non-Ad, other histological types; VPI, visceral pleural invasion.
* $p<0.05$.

(Table 2a). In patients with p-stage IB tumors, men, ever smokers, non-adenocarcinoma, the presence of BVI, and the presence of lymphatic permeation were significant poor prognostic factors. Multivariate survival analysis showed that the presence of BVI was a significant independent prognostic factor, as well as men and the presence of lymphatic permeation (HR = 2.347, $p=0.0088$) (Table 2b).

Thus, we analyzed the OS of p-stage IA patients stratified by tumor size (≤2 cm, T1a; >2 cm, T1b) and BVI status (presence or absence) (Fig. 3a), and we also analyzed the OS of p-stage IB patients stratified by BVI status (Fig. 3b).

In the p-stage IA patient cohort, subgroup analysis of the patients revealed 5-year OS rates of 94.5%, 87.1%, 82.7%, and 65.9% for patients with T1a/non-BVI, T1a/BVI, T1b/non-BVI, and T1b/BVI, respectively (Fig. 3a). The differences in survival were statistically significant between patients with T1a/BVI and T1a/non-BVI tumors, and between patients with T1b/BVI and T1b/non-BVI tumors ($p<0.001$ and $p=0.034$, respectively). There was no significant difference in the survival rates between the T1a/BVI and T1b/non-BVI subgroups ($p=0.2604$). On the other hand, in the p-stage IB patient cohort, subgroup analysis of the patients revealed 5-year OS rates of 90.3% and 61.5% for patients with T2a/non-BVI and T2a/BVI tumors, respectively, with statistically significant difference ($p<0.001$) (Fig. 3b).

We also analyzed the prognosis of T1b, T2a and T2b tumors (Table 3). There was no significant difference in survival between the patients with T1b/non-BVI and T2a/non-BVI tumors ($p=0.0753$). There was no significant difference in survival between patients with T1b/BVI and T2a/BVI tumors, and between patients with T2a/BVI and T2b tumors ($p=0.7364$ and $p=0.2394$, respectively).

The patients with T1a/BVI tumors had lower RFS than the patients with T1b/non-BVI, with no significant difference ($p=0.2090$) (Fig. 3c). However, in RFS curves, similar relationships to OS curves were observed among these subgroups with each pathological stage tumor (Fig. 3c and d).

Table 2a
Univariate and multivariate analyses of prognostic factors in stage IA patients.

Variable	UVA	MVA		
	p-Value	Hazard ratio	95%CI	*p*-Value
Sex: men (vs women)	0.0159*	1.205	0.5921–2.451	0.6076
Age: >70 (vs ≤70)	0.0125*	1.852	1.091–3.145	0.0226*
Smoking history: ever smoker (vs never smoker)	0.0059*	1.290	0.601–2.770	0.5134
Operation procedure: bilobectomy (vs lobectomy)	NS (0.1968)		Not included in MVA	
Tumor location	NS (0.387)		Not included in MVA	
Tumor size: >2 cm (vs ≤2 cm)	0.0007*	2.096	1.266–3.472	0.0040*
Histologic type: non-Ad (vs Ad)	<0.0001*	2.899	1.624–5.176	0.0003*
BVI: present (vs absent)	0.0001*	2.591	1.529–4.386	0.0004*
Lymphatic permeation: present (vs absent)	NS (0.4553)		Not included in MVA	

UVA, univariate analysis; MVA, multivariate analysis; Ad, adenocarcinoma; non-Ad, other histological types; BVI, blood vessel invasion.
* $p < 0.05$.

Table 2b
Univariate and multivariate analyses of prognostic factors in stage IB patients.

Variable	UVA	MVA		
	p-Value	Hazard ratio	95%CI	*p*-Value
Sex: men (vs women)	<0.0001*	3.690	1.475–9.259	0.0052*
Age: >70 (vs≤70)	NS (0.7117)		Not included in MVA	
Smoking history: ever smoker (vs never smoker)	0.0007*	1.016	0.475–2.037	0.9657
Operation procedure: bilobectomy (vs lobectomy)	NS (0.5782)		Not included in MVA	
Tumor location	NS (0.6533)		Not included in MVA	
Tumor size: >3 cm (vs≤3 cm)	NS (0.0665)		Not included in MVA	
Histologic type: non-Ad (vsAd)	0.0006*	1.226	0.716–2.101	0.4575
BVI: present (vs absent)	<0.0001*	2.347	1.239–4.464	0.0088*
Lymphatic permeation: present (vs absent)	<0.0001*	2.288	1.279–4.082	0.0053*
VPI: present (vs absent)	NS (0.8943)		Not included in MVA	

UVA, univariate analysis; MVA, multivariate analysis; Ad, adenocarcinoma; non-Ad, other histological types; BVI, blood vessel invasion; VPI, visceral pleural invasion.
* $p < 0.05$.

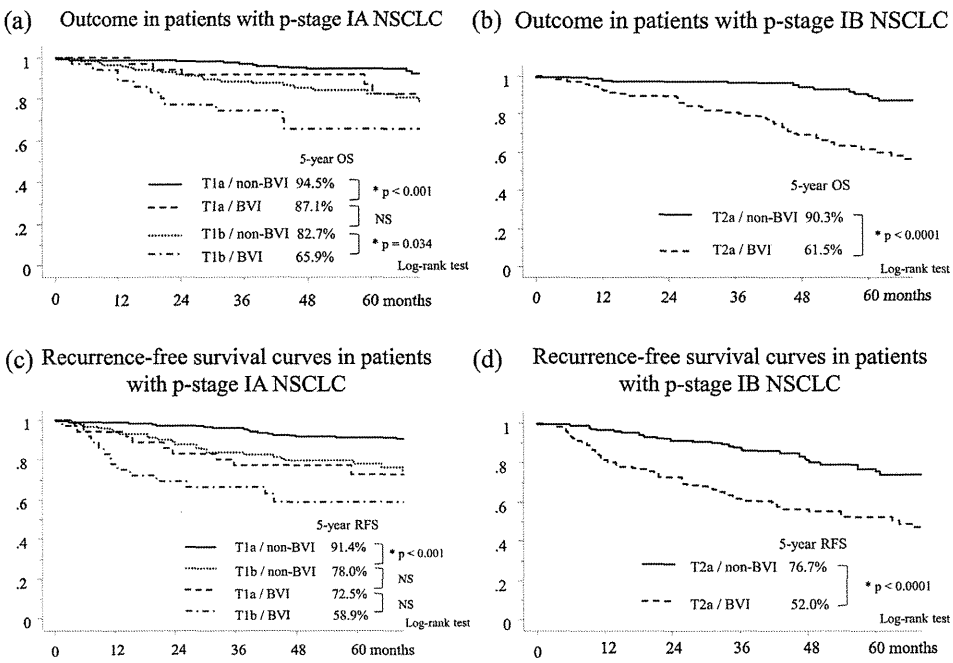

Fig. 3. (a) Survival curves and 5-year overall survival (OS) rates stratified by T-factor (T1a or T1b) and blood vessel invasion (BVI) status in patients with p-stage IA non-small cell lung cancer (NSCLC). (b) Survival curves and 5-year OS rates stratified by BVI status in patients with p-stage IB NSCLC. (c) Recurrence-free survival (RFS) curves and 5-year RFS rates stratified by T-factor (T1a or T1b) and blood vessel invasion (BVI) status in patients with p-stage IA non-small cell lung cancer (NSCLC). (d) RFS curves and 5-year RFS rates stratified by BVI status in patients with p-stage IB NSCLC. *$p < 0.05$.

Table 3
Proposal on incorporating vascular invasion into T classification.

Group	n	5yOS	p-value	7th Edition stage (N0M0)	Our proposal stage (N0M0)
T1a/non-BVI	227	94.5%	< 0.0001	IA	IA
T1a/BVI	38	87.5 %	NS (0.2604)	IA	**IB**
T1b/non-BVI	125	82.7%	0.034	IA	**IB**
T1b/BVI	39	65.9%	0.0002	IA	**IIA**
T2a/non-BVI	145	90.9%	< 0.0001	IB	IB
T2a/BVI	130	61.8%	NS (0.2394)	IB	**IIA**
T2b	36	68.7%		IIA	IIA

NS (0.0753)
NS (0.7364)

T-factor and stage in bold in our proposal differ from those in the 7th edition classification. Non-BVI, without blood vessel invasion; BVI, with blood vessel invasion; 5y OS, 5-year overall survival rate.

4. Discussion

The TNM stage classification was developed as a benchmark for prognosis and treatment options. For patients with stage I lung cancer, however, survival outcomes vary, thus stage I NSCLC comprises a heterogeneous group with different prognoses [13]. BVI has been shown to be a strong independent predictor for p-stage I disease as a variable for analyses [7,9–12,14], with only few exceptions [15,16]. In several other malignancies, BVI has similarly been shown to predict poor outcome [17–19], and its value has been commonly recognized to the point that it is included in the AJCC staging system for testicular cancer [20]. The first studies about the prognostic role of BVI in lung cancer date back to the late 1950s [21]. Despite the numerous reports of BVI as a negative prognostic factor and that BVI has been taken into account in the supplementary TNM staging, BVI has not yet been incorporated into the T classification component.

One possible reason may be that there is a lack of standardization of evaluating BVI. Many variations regarding the method of BVI assessment exist, although in most studies BVI was defined as the presence of neoplastic structures inside the lumen of a vessel. Ichinose et al. reported that venous invasion was one of the significant prognostic factors among patients with completely resected NSCLC [22]. On the other hand, arterial invasion was reported to be strongly associated with 5-year survival in patients with stage I NSCLC [23]. Arterial and venous invasion has not yet been studied pathologically separately in our institute, because discrimination was not always possible. Some studies evaluated BVI by staining with hematoxylin and eosin alone or in combination with EvG stain or by staining with Victoria blue hematoxylin and eosin, which can lead to significant heterogeneity. The reported detection rates of BVI in pathological stage I NSCLC case without any elastic fiber stains were 11–17% [15,24]. In contrast, those with elastic fiber stains ranged from 21% to 56% and were higher than those without [9,16,25]. We uniformly used hematoxylin and eosin and EvG stains on all tumors and the detection rate was 28.9% for patients with pathological stage I, which was similar to previous studies [9,16,25]. These findings suggest that elastic fiber staining helps pathologists to identify BVI more accurately in almost all cases. In the latest 7th edition of the TNM classification, VPI is clearly defined and T1 tumors remain to be upgraded to T2a when the visceral pleural elastic layer is invaded. Elastic fiber staining is also helpful in identifying VPI. We therefore recommend the routine use of elastic fiber stains in pathological evaluations of lung cancer, not only for VPI determination, as recommended in the TNM classification, but also for BVI determination, especially in patients with stage I NSCLC, to reflect more accurate, prognosis.

In this series, we showed that the 5-year OS rate of BVI patients was significantly lower than that of non-BVI patients (Table 3). These results indicate that T1a tumors with BVI should be classified as T1b, T1b tumors with BVI as T2a, and T2a tumors with BVI as T2b. This would also be consistent with other tumors with BVI being upgraded to the next T level. Our proposal on incorporating BVI into T classification can be framed to yield a better staging system for stage I NSCLC.

BVI is one of the steps leading to metastatic diffusion, and this may be the reason that BVI is associated with a poorer prognosis. Tumor cells from the primary neoplasm may penetrate these new vessels and escape from the primary site to distant organs. The relationship between tumor vessels, intravascular tumor cell invasion, and metastases has been studied in animal models [26]. In our series, there were 44 patients and 74 with recurrence in stage IA and stage IB, respectively. Among these patients, the patterns of initial recurrence included distant metastasis in 31 patients (70.5%) and in 58 (78.3%), respectively (data not shown). Classified by BVI status, recurrence developed in 17 (23.3%) of stage IA patients with BVI, and recurrence in 27 (7.7%) of these patients with non-BVI, with significant difference ($p = 0.0004$, data not shown). However, there were high rates of distant metastasis in both groups, and there were no significant differences in initial recurrence patterns. In the stage IB patients, recurrence developed in 51 (39.8%) of patients with BVI, and recurrence in 23 (16.1%) of patients with non-BVI, with a significant difference ($p < 0.0001$, data not shown). However, there were high rates of distant metastasis in both groups, and there were no significant differences in initial recurrence patterns. Surgery is considered to be the standard treatment for early-stage NSCLC. However, distant metastasis occurred in nearly 60–70% of recurrence patients with stage I NSCLC after complete resection [27,28]. Micrometastasis of the tumor is generally regarded as the cause of recurrence; therefore systemic chemotherapy after surgery is a rational strategy to reduce the risk of recurrence and metastasis.

Recent randomized controlled trials have demonstrated the survival benefit varied with stage and the usefulness of platinum-based adjuvant chemotherapy in p-stage II to IIIA NSCLC patients [29–31]. For stage IB adenocarcinoma patients, based on a large adjuvant trial on oral uracil-tegafur (UFT), UFT adjuvant

chemotherapy is recommended as the standard treatment in Japan [32]. Although surgery alone remains the standard treatment for patients with stage IA disease, recent Japanese studies also showed that oral UFT may improve survival in patients with p-stage IA showing a tumor size of 2–3 cm [32,33]. Recently, the proposed IASLC/ATS/ERS classification of lung adenocarcinoma identified histological categories with prognostic differences that may be helpful in identifying candidates for adjuvant therapy and was associated with BVI [34,35], but there might be some lack of preparation to incorporate the classification into the staging system. In the present study, when we divided the study population stratified by BVI, the patients with BVI have worse survival than those without BVI (Table 3). This classification can incorporate the prognostic impact of BVI status into the 7th edition T classification reasonably well, and patients with each stage of NSCLC with BVI may therefore be good candidates for adjuvant chemotherapy. BVI is an important parameter to venture postoperative poor prognostic groups in a strategical staging system.

Due to the retrospective analysis in a single institute, which evaluated cases from 1999, and due to a small sample size compared with T2b patients, making it impossible to draw any statistically significant conclusions in these subgroups, our proposal is not complete. Furthermore, it is difficult to evaluate BVI in the clinical staging setting. However, our data clearly indicate that BVI has a very strong prognostic impact. Prospective multi-institutional studies are mandatory to further validate the prognosis of BVI in resected stage I NSCLC.

In conclusion, despite the limitations mentioned above, we have demonstrated the prognostic power of BVI as a single independent pathologic marker for NSCLC, and our results have indicated that T1a tumors with BVI should, unlike in the 7th TNM classification, be classified as T1b, T1b tumors with BVI as T2a, and T2a tumors with BVI as T2b. In future revisions of the TNM staging system, we recommend the routine use of elastic tissue stains in pathological evaluations of lung cancer for BVI determination, and we believe that tumors with BVI should be upstaged to the above T stages. As this will affect staging criteria, additional studies employing standard methodology to assess BVI are needed to further clarify the underlying reasons why tumors with BVI have an unfavorable prognosis.

Funding

This study was supported by grants from the Ministry of Education, Culture, Sports, Science and Technology (Grant no. 21791332) and the Ministry of Health, Labor and Welfare (Grant no. 22101601), and by a Grant-in-Aid for Young Scientists (B) from Japan Society for the Promotion of Science (KAKENHI 24791474).

Conflict of interest statement

None declared.

Acknowledgements

We are indebted to Ms. Maya Vardaman, Associate Professor Edward F. Barroga, and Professor J. Patrick Barron, Chairman of the Department of International Medical Communications of Tokyo Medical University, for their editorial review of the English manuscript.

References

[1] Sawabata N, Miyaoka E, Asamura H, Nakanishi Y, Eguchi K, Mori M, et al. Japanese lung cancer registry study of 11,663 surgical cases in 2004: demographic and prognosis changes over decade. J Thorac Oncol 2011;6:1229–35.
[2] Asamura H, Goya T, Koshiishi Y, Sohara Y, Eguchi K, Mori M, et al. A Japanese Lung Cancer Registry study: prognosis of 13,010 resected lung cancers. J Thorac Oncol 2008;3:46–52.
[3] Agarwal M, Brahmanday G, Chmielewski GW, Welsh RJ, Ravikrishnan KP. Age, tumor size, type of surgery, and gender predict survival in early stage (stage I and II) non-small cell lung cancer after surgical resection. Lung Cancer 2010;68:398–402.
[4] Kawai H, Tada A, Kawahara M, Nakai K, Maeda H, Saitou R, et al. Smoking history before surgery and prognosis in patients with stage IA non-small-cell lung cancer – a multicenter study. Lung Cancer 2005;49:63–70.
[5] Okada M, Sakamoto T, Nishio W, Uchino K, Tsubota N. Characteristics and prognosis of patients after resection of nonsmall cell lung carcinoma measuring 2 cm or less in greatest dimension. Cancer 2003;98:535–41.
[6] Shimada Y, Saji H, Yoshida K, Kakihana M, Honda H, Nomura M, et al. Pathological vascular invasion and tumor differentiation predict cancer recurrence in stage IA non-small-cell lung cancer after complete surgical resection. J Thorac Oncol 2012;7:1263–70.
[7] Suzuki K, Nagai K, Yoshida J, Nishimura M, Takahashi K, Yokose T, et al. Conventional clinicopathologic prognostic factors in surgically resected nonsmall cell lung carcinoma. A comparison of prognostic factors for each pathologic TNM stage based on multivariate analyses. Cancer 1999;86:1976–84.
[8] Saji H, Tsuboi M, Yoshida K, Kato Y, Nomura M, Matsubayashi J, et al. Prognostic impact of number of resected and involved lymph nodes at complete resection on survival in non-small cell lung cancer. J Thorac Oncol 2011;6:1865–71.
[9] Ogawa J, Tsurumi T, Yamada S, Koide S, Shohtsu A. Blood vessel invasion and expression of sialyl Lewisx and proliferating cell nuclear antigen in stage I non-small cell lung cancer. Relation to postoperative recurrence. Cancer 1994;73:1177–83.
[10] Tsuchiya T, Akamine S, Muraoka M, Kamohara R, Tsuji K, Urabe S, et al. Stage IA non-small cell lung cancer: vessel invasion is a poor prognostic factor and a new target of adjuvant chemotherapy. Lung Cancer 2007;56:341–8.
[11] Ruffini E, Asioli S, Filosso PL, Buffoni L, Bruna MC, Mossetti C, et al. Significance of the presence of microscopic vascular invasion after complete resection of stage I-II pT1-T2N0 non-small cell lung cancer and its relation with T-Size categories: did the 2009 7th edition of the TNM staging system miss something? J Thorac Oncol 2011;6:319–26.
[12] Naito Y, Goto K, Nagai K, Ishii G, Nishimura M, Yoshida J, et al. Vascular invasion is a strong prognostic factor after complete resection of node-negative non-small cell lung cancer. Chest 2010;138:1411–7.
[13] Bergman P, Brodin D, Lewensohn R, de Petris L. Validation of the 7th TNM classification for non-small cell lung cancer: A retrospective analysis on prognostic implications for operated node-negative cases. Acta Oncol 2012 [Epub ahead of print].
[14] Maeda R, Yoshida J, Ishii G, Hishida T, Nishimura M, Nagai K. Prognostic impact of intratumoral vascular invasion in non-small cell lung cancer patients. Thorax 2010;65:1092–8.
[15] Poleri C, Morero JL, Nieva B, Vazquez MF, Rodriguez C, de Titto E, et al. Risk of recurrence in patients with surgically resected stage I non-small cell lung carcinoma: histopathologic and immunohistochemical analysis. Chest 2003;123:1858–67.
[16] Brechot JM, Chevret S, Charpentier MC, Appere de Vecchi C, Capron F, Prudent J, et al. Blood vessel and lymphatic vessel invasion in resected nonsmall cell lung carcinoma. Correlation with TNM stage and disease free and overall survival. Cancer 1996;78:2111–8.
[17] Du C, Zhou Y, Cai H, Zhao G, Fu H, Shi YQ. Poor prognostic factors in patients with stage I gastric cancer according to the seventh edition TNM classification: a comparative analysis of three subgroups. J Surg Oncol 2012;105:323–8.
[18] Sakuragi N, Takeda N, Hareyama H, Fujimoto T, Todo Y, Okamoto K, et al. A multivariate analysis of blood vessel and lymph vessel invasion as predictors of ovarian and lymph node metastases in patients with cervical carcinoma. Cancer 2000;88:2578–83.
[19] Mirza AN, Mirza NQ, Vlastos G, Singletary SE. Prognostic factors in node-negative breast cancer: a review of studies with sample size more than 200 and follow-up more than 5 years. Ann Surg 2002;235:10–26.
[20] Krege S, Beyer J, Souchon R, Albers P, Albrecht W, Algaba F, et al. European consensus conference on diagnosis and treatment of germ cell cancer: a report of the second meeting of the European Germ Cell Cancer Consensus group (EGCCCG): part I. Eur Urol 2008;53:478–96.
[21] Collier FC, Enterline HT, Kyle RH, Tristan TT, Greening R. The prognostic implications of vascular invasion in primary carcinomas of the lung; a clinicopathologic correlation of two hundred twenty-five cases with one hundred per cent follow-up. AMA Arch Pathol 1958;66:594–603.
[22] Ichinose Y, Yano T, Asoh H, Yokoyama H, Yoshino I, Katsuda Y. Prognostic factors obtained by a pathologic examination in completely resected non-small-cell lung cancer. An analysis in each pathologic stage. J Thorac Cardiovasc Surg 1995;110:601–5.
[23] Pechet TT, Carr SR, Collins JE, Cohn HE, Farber JL. Arterial invasion predicts early mortality in stage I non-small cell lung cancer. Ann Thorac Surg 2004;78:1748–53.
[24] Harpole Jr DH, Herndon 2nd JE, Young Jr WG, Wolfe WG, Sabiston Jr DC. Stage I nonsmall cell lung cancer. A multivariate analysis of treatment methods and patterns of recurrence. Cancer 1995;76:787–96.
[25] Ichinose Y, Yano T, Yokoyama H, Inoue T, Asoh H, Katsuda Y. The correlation between tumor size and lymphatic vessel invasion in resected peripheral stage

I non-small-cell lung cancer. A potential risk of limited resection. J Thorac Cardiovasc Surg 1994;108:684–6.
[26] Liotta LA, Kleinerman J, Saidel GM. Quantitative relationships of intravascular tumor cells, tumor vessels, and pulmonary metastases following tumor implantation. Cancer Res 1974;34:997–1004.
[27] Rena O, Oliaro A, Cavallo A, Filosso PL, Donati G, Di Marzio P, et al. Stage I non-small cell lung carcinoma: really an early stage? Eur J Cardiothorac Surg 2002;21:514–9.
[28] Hung JJ, Jeng WJ, Hsu WH, Chou TY, Huang BS, Wu YC. Predictors of death, local recurrence, and distant metastasis in completely resected pathological stage-I non-small-cell lung cancer. J Thorac Oncol 2012;7:1115–23.
[29] Arriagada R, Bergman B, Dunant A, Le Chevalier T, Pignon JP, Vansteenkiste J. Cisplatin-based adjuvant chemotherapy in patients with completely resected non-small-cell lung cancer. N Engl J Med 2004;350:351–60.
[30] Douillard JY, Rosell R, De Lena M, Carpagnano F, Ramlau R, Gonzales-Larriba JL, et al. Adjuvant vinorelbine plus cisplatin versus observation in patients with completely resected stage IB-IIIA non-small-cell lung cancer (Adjuvant Navelbine International Trialist Association [ANITA]): a randomised controlled trial. Lancet Oncol 2006;7:719–27.
[31] Winton T, Livingston R, Johnson D, Rigas J, Johnston M, Butts C, et al. Vinorelbine plus cisplatin vs. observation in resected non-small-cell lung cancer. N Engl J Med 2005;352:2589–97.
[32] Kato H, Ichinose Y, Ohta M, Hata E, Tsubota N, Tada H, et al. A randomized trial of adjuvant chemotherapy with uracil-tegafur for adenocarcinoma of the lung. N Engl J Med 2004;350:1713–21.
[33] Hamada C, Tsuboi M, Ohta M, Fujimura S, Kodama K, Imaizumi M, et al. Effect of postoperative adjuvant chemotherapy with tegafur-uracil on survival in patients with stage IA non-small cell lung cancer: an exploratory analysis from a meta-analysis of six randomized controlled trials. J Thorac Oncol 2009;4:1511–6.
[34] Yoshizawa A, Motoi N, Riely GJ, Sima CS, Gerald WL, Kris MG, et al. Impact of proposed IASLC/ATS/ERS classification of lung adenocarcinoma: prognostic subgroups and implications for further revision of staging based on analysis of 514 stage I cases. Mod Pathol 2011;24:653–64.
[35] Russell PA, Wainer Z, Wright GM, Daniels M, Conron M, Williams RA. Does lung adenocarcinoma subtype predict patient survival? A clinicopathologic study based on the new International Association for the Study of Lung Cancer/American Thoracic Society/European Respiratory Society international multidisciplinary lung adenocarcinoma classification. J Thorac Oncol 2011;6:1496–504.

CHEST Original Research
LUNG CANCER

A Proposal for Combination of Total Number and Anatomical Location of Involved Lymph Nodes for Nodal Classification in Non-small Cell Lung Cancer

Hisashi Saji, MD, PhD; Masahiro Tsuboi, MD, PhD; Yoshihisa Shimada, MD, PhD; Yasufumi Kato, MD, PhD; Koichi Yoshida, MD, PhD; Masaharu Nomura, MD, PhD; Jun Matsubayashi, MD, PhD; Toshitaka Nagao, MD, PhD; Masatoshi Kakihana, MD, PhD; Jitsuo Usuda, MD, PhD; Naohiro Kajiwara, MD, PhD; Tatsuo Ohira, MD, PhD; and Norihiko Ikeda, MD, PhD

Background: **We previously reported the prognostic impact of the number of involved lymph nodes (LNs) on survival in non-small cell lung cancer (NSCLC). However, it remains unknown whether the total number or anatomic location of involved LNs is a superior prognostic factor.**
Methods: **A total of 689 patients with NSCLC who underwent complete resection involving dissection of the hilar and mediastinal LNs with curative intent of ≥ 10 LNs were enrolled. The association between the total number of LNs (nN) involved and survival was assessed by comparison with the anatomic location of LN involvement (pathologic lymph node [pN]), the present nodal category.**
Results: **We classified the patients into five categories according to the combined pN and nN status as follows: pN0-nN0, pN1-nN1-3, pN1-nN4−, pN2-nN1-3, and pN2-nN4. Although there was no statistically significant difference between the pN1-nN4− and pN2-nN1-3 categories, pN2-nN1-3 had better prognoses than pN1-nN4−. On multivariate analysis, the nN category was an independent prognostic factor for overall survival and disease-free survival (vs nN4−; the hazard ratios of nN0 and nN1-3 for overall survival were 0.223 and 0.369, respectively, $P < .0001$ for all), similar to the pN category. We propose a new classification based on a combination of the pN and nN categories: namely, N0 becomes pN0-nN0, the N1 category becomes pN1-nN1-3, the N2a category becomes pN2-nN1-3 + pN1-nN4−, and the N2b category becomes pN2-nN4. Each survival curve was proportional and was well distributed among the curves.**
Conclusions: **A combined anatomically based pN stage classification and numerically based nN stage classification is a more accurate prognostic determinant in patients with NSCLC, especially in the prognostically heterogeneous pN1 and pN2 cases. Further large-scale international cohort validation analyses are warranted.** ***CHEST 2013; 143(6):1618–1625***

Abbreviations: DFS = disease-free survival; LN = lymph node; nN = number of lymph nodes; NSCLC = non-small cell lung cancer; OS = overall survival; pN = pathologic lymph node; pT = pathologic tumor

Various pathologic and molecular markers have been assessed regarding their usefulness in identifying patients at high risk for recurrence. However, the TNM system remains the most important determinant of staging. Because the prognosis of lung cancer is directly proportional to the presence of lymph node (LN) metastasis, accurate LN assessment is crucial in determining treatment. Accurate staging of non-small cell lung cancer (NSCLC) requires assessment of the hilar and mediastinal LNs with pathologic evaluation. However, the present nodal classification still contains some limitations particularly concerning heterogeneous pN1 and pN2 disease and the lack of a clear biologic definition of the distinguishing of N1 and N2.[1-4]

For editorial comment see page 1527